Eur. Phys. J. B **41**, 213–217 (2004)
DOI: 10.1140/epjb/e2004-00312-9

**THE EUROPEAN
PHYSICAL JOURNAL B**

Magnetocaloric effect in ordered double-perovskite Ba_2FeMoO_6 synthesized using wet chemistry

W. Zhong[1,a], X.L. Wu[1], N.J. Tang[1], W. Liu[1], W. Chen[2], C.T. Au[3], and Y.W. Du[1]

[1] National Laboratory of Solid State Microstructures and Jiangsu Provincial Laboratory for Nano Technology, Nanjing University, Nanjing 210093, P.R. China
[2] Department of Physics, Heibei Normal University, Shijiazhuang 050091, P.R. China
[3] Chemistry Department and Center for Surface Analysis and Research, Hong Kong Baptist University, Kowloon Tong, Hong Kong

Received 23 February 2004 / Received in final form 3 June 2004

Abstract. Double perovskite Ba_2FeMoO_6 has been prepared by a wet chemistry method and its magnetocaloric effect has been studied. The Ba_2FeMoO_6 sample, consisting of crystallites with diameter of 130 nm and average aspect ratio of 15, exhibits a sharp magnetic transition. The maximum of the magnetic entropy change peaks at its Curie temperature (340 K), and a large magnetic entropy change (∼1.54 J/kg K, or ∼0.081 J/mol (atoms) K) is obtained upon 10 kOe applied magnetic field change. For comparison, the magnetic properties of Ba_2FeMoO_6 prepared by a conventional solid-state reaction was also investigated.

PACS. 75.30.Sg Magnetocaloric effect, magnetic cooling – 82.80.-d Chemical analysis and related physical methods of analysis – 81.05.Mh Cermets, ceramic and refractory composites

1 Introduction

Half-metallic compounds, i.e. materials with only one spin direction present at the Fermi level, are interesting for their potential applications at room temperature in spin electronics. In this sense, oxides with high spin polarization and high Curie temperatures are desirable. Recently, double-perovskite oxides of the type $A_2B'B''O_6$, being also half-metallic ferromagnets, have received a great deal of attention because they display a substantial magnetoresistance and their Curie temperature is well above that of optimally doped simple manganite perovskites (such as $La_{2/3}Ca_{1/3}MnO_3$) [1]. Usually, A is a large cation capable of 12-fold coordination with oxygen while B' and B'' are different smaller cations suitable for octahedral coordination [2]. Among double perovskites, Fe-based oxides A_2FeMoO_6 (A = Sr, Ba, Ca, ...) have attracted much attention as a novel class of magnetoresistive oxides, since the low-field tunneling-type magnetoresistance effect was found in Sr_2FeMoO_6 (SFMO) at room temperature [1]. It has been suggested that this compound has a double perovskite structure with alternately ordered Fe^{3+} ($3d^5$, $S = 5/2$) and Mo^{5+} ($4d^1$, $S = 1/2$) ions in the cubic ABO_3 perovskite [3]. The Fe and Mo sublattices are ferromagnetically coupled within each sublattice, while the two sublattices are supposed to be antiferromagnetically coupled. This gives rise to an $S = 2$ state and thus a saturation magnetization $M_S = 4\mu_B$ ($T = 0$ K) is predicted. However, the M_S values of bulk materials reported so far are systematically much smaller than the predicted $4\mu_B$ value. This difference between ideal and actual materials is believed to have its main origin in the lack of cationic ordering in the Fe/Mo sublattices. Since the ionic sizes of Fe^{3+} and Mo^{5+} are similar, there is a finite concentration of antisite defects in A_2FeMoO_6, which interchange the positions of Fe and Mo in a random fashion. Each cation Fe that is misplaced in a Mo position is called an antisite (AS) defect. From the effects of AS defects on the saturation magnetization, it can be infered that since the sublattices Fe and Mo are antiferromagnetically arranged, each antisite contributes to a certain decrease of the saturation moment of the sample [4,5].

Many researchers have reported structural, magnetization, resistivity, Hall effect, specific heat and magnetic aftereffect of Fe-based double perovskite transition-metal oxides [6–20]. The properties of the double perovskites A_2FeMoO_6 (A = Ca, Sr and Ba) are thought to critically depend on the concentration of AS defects, which depends on the preparation method and synthesis conditions, such as heat-treatment temperature, time, and atmosphere. Most double perovskite materials reported previously were prepared by conventional solid-state reactions. Samples synthesized using conventional techniques frequently have

---

[a] e-mail: `wzhong@ufp.nju.edu.cn`

isotropic grains with micrometer-scale size. Furthermore, to our knowledge, no studies have been carried on the magnetocaloric effect (MCE) of double perovskite transition-metal oxides. In the present work, we synthesized double perovskite Ba_2FeMoO_6 having high aspect ratio crystallites using wet chemistry, and studied its magnetocaloric effect above room temperature. For comparison, the structure, morphology and magnetic properties (including magnetocaloric effect) of Ba_2FeMoO_6 prepared by a conventional solid-state reaction were also investigated.

2 Experimental

Double perovskite Ba_2FeMoO_6 was prepared by a wet chemistry method as follows: stoichiometric amounts of $(NH_4)_6Mo_7O_{24}\cdot 4H_2O$, $Fe(NO_3)_3\cdot 9H_2O$ and $BaCO_3$ were dissolved in dilute HNO_3 solution at 333 K. Then suitable amounts of citric acid and ethylene glycol as coordinate agent were added in the reactor and a completely homogeneous light yellow transparent solution was achieved after heating at 343 K for 20 minutes. This solution was subjected to evaporation until a highly viscous residual was formed and a gel was developed during heating at 443 K. The gel was thermally treated at 773 K for 5 hours to decompose the organic precursor. After grinding, the sample was calcined in a stream of 7% H_2/Ar at 1273 K for 5 h and furnace cooled.

In order to study the influence of preparation methods on the structure and properties of double perovskites, Ba_2FeMoO_6 was also prepared by a conventional solid-state reaction method as follows: powders of $BaCO_3$, Fe_2O_3, and MoO_3 were mixed at stoichiometric ratios. Oxide mixtures were milled by high-energy ball milling for 5 h and then preheated at 873 K for 5 h under air. After further milling for another 5 h, the sample was sintered at 1273 K under an Ar/H_2 (7%) atmosphere for 10 h. The process was repeated three times in order to complete the reaction.

It is noteworthy that in order to guarantee a precise sample composition, the sintering conditions must be carefully observed for both preparation methods. Higher temperatures and/or longer sintering times could produce different sample compositions because of the possibility of molybdenum oxide evaporation.

Phase identification and structural analysis were examined by X-ray powder diffraction (XRD) with Cu $K\alpha$ radiation (Model D/Max-RA, Rigaku, Japan). The metal content in the sintered sample was determined by induced coupled plasma (ICP) spectroscopy (Model 1100 + 2000, Jarrell-Ash, USA). The oxygen content was also estimated by deducting the metal content from the weighed sample. The morphology of Ba_2FeMoO_6 was examined directly by transmission electron microscopy [(TEM), Model JEM-200 CX, JEOL, Japan] and scanning electron microscopy [(SEM), JSM-5610 LV, JEOL, Japan]. Magnetization (M) versus temperature (T) and magnetization versus magnetic field (H) curves were measured by a vibrating sample magnetometer [(VSM), Model PAR 155, USA]. Curie temperature (T_C) was determined from the M-T curves. Magnetization of samples was measured in an isothermal regime under an applied magnetic field varying from 0 to 10 kOe. In the vicinity of T_C, isothermal M-H curves were obtained by a step of 3 or 5 K.

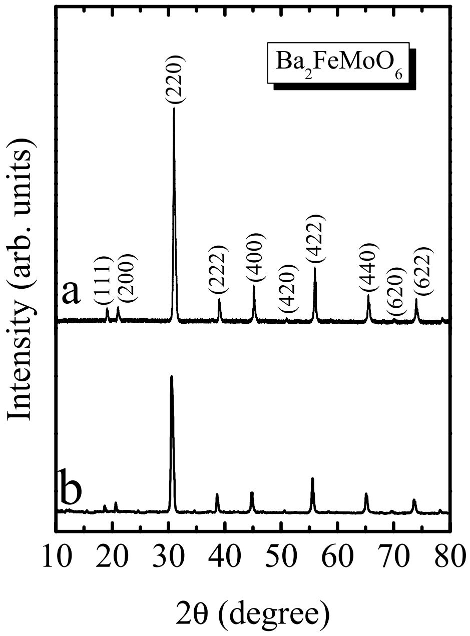

Fig. 1. XRD patterns of the two Ba_2FeMoO_6 samples prepared by (a) wet chemistry and (b) solid-state reaction.

3 Results and discussion

The results of ICP indicate that the actual metal and oxygen content for both the samples prepared by wet chemistry, and the solid state reaction methods explored in this work, is practically equal to the nominal value. The X-ray diffraction patterns of the two samples prepared by wet chemistry and solid state reaction methods are shown in Figure 1. Both of them are single phase of Ba_2FeMoO_6 without any detectable secondary phase, but the intensities of some peaks vary with preparation method. The diffraction peaks are indexed with respect to the cubic structure with a space group of $Fm3m$, where the unit cell has parameter $a = 0.8071$ (3) and $a = 0.8078$ (3) nm for samples prepared by wet chemistry and solid state reaction, respectively. These lattice parameters are similar to the value (0.80747 nm) reported by Kim et al. [9] but smaller than the value (0.8062 nm) obtained by Borges et al. [19] The concentration of antisite (AS) defects of the Fe and Mo arrangement were obtained from Rietveld refinements. The AS concentration is defined as the ratio of the concentration of Fe cations in Mo positions divided by the total Fe cations. Therefore, AS = 50% corresponds to a totally disordered double perovskite. The AS defect concentrations were estimated to be 2% and 9% for samples prepared by wet chemistry and solid state reaction, respectively. For the wet chemistry method used in our

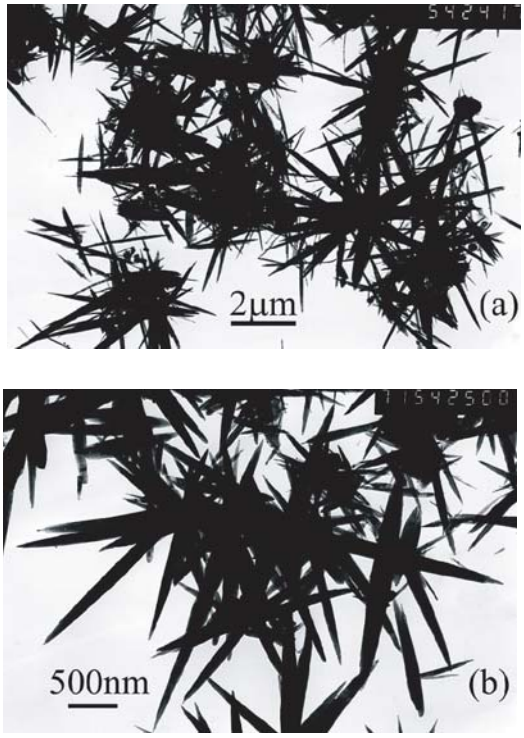

Fig. 2. Representative TEM images at two different magnifications of the Ba_2FeMoO_6 prepared by wet chemistry.

experiment, the reactant is a heteropolymer of molybdates. When the reactant is preheated, it becomes a mixture of metal oxides, which are fully uniformly mixed at the atomic scale. Thus it is easier to transform into Ba_2FeMoO_6 with a high order parameter.

Figures 2a and b show representative TEM images of Ba_2FeMoO_6 prepared by wet chemistry. One can see that the sample exhibits bullrush-like crystallites with diameter of 130 nm and high aspect ratio larger than 15. Figure 3 presents a typical micrograph of Ba_2FeMoO_6 prepared by solid state reaction. One can observe that the sample consists of inhomogeneous aggregates of granules with different shape and size.

The ferromagnetic ordering transition temperature, defined as the temperature at which the $dM/dT \sim T$ curve reaches a minimum, has been extracted from the low field (1 kOe) magnetization versus temperature. The T_C values vary little for the two samples. Figure 4 displays the temperature dependence of magnetization M for the two samples Ba_2FeMoO_6. The magnetization was measured upon warming in a 10 kOe field after cooling to 100 K in zero field. The M at 173 K in a 10 kOe field is 37.3 emu/g (3.49 μ_B/per formula unit) for Ba_2FeMoO_6 prepared by wet chemistry. As can be seen, the magnetization of the sample prepared by solid state reaction is lower than that of the sample prepared by wet chemistry. Further investigations into the magnetic behavior at lower temperature are in progress. Although the magnetization at 173 K is not saturated, the tendency of saturation magneticzation (M_S) may be estimated from Figure 4. This decrease of magnetization would be due to antisite defects resulting from the partial disorder of Fe and Mo ions among the B'/B'' sublattices. Balcells et al. [2] observed that the experimental saturation magnetization had an almost linear dependence on the AS concentration. Monte Carlo calculations of Ogale et al. [4] have also predicted a reduction of magnetization as a function of the AS defect concentration:

$$M_S\,(\mu_B/\text{f.u.}) = 4{-}8 \times (AS). \quad (1)$$

Sakuma et al. [21] discussed the dependence of the spontaneous magnetization (M_0) on the order parameter (x) using two models considering the local magnetic interaction between ions on the B sites, and reported the relationships

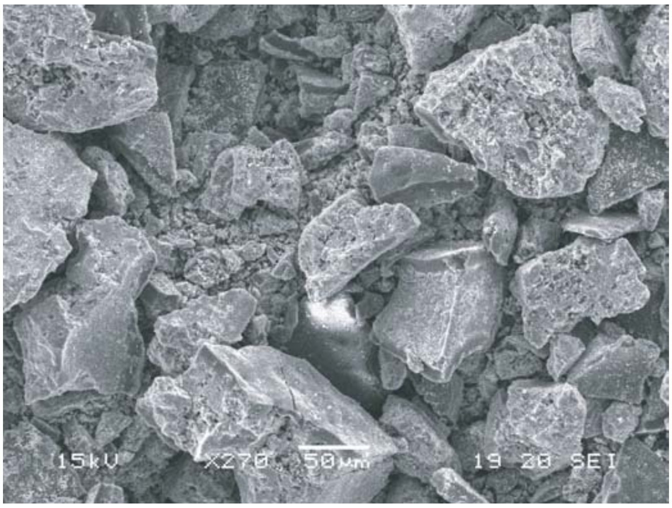

Fig. 3. SEM image of the Ba_2FeMoO_6 prepared by solid-state reaction.

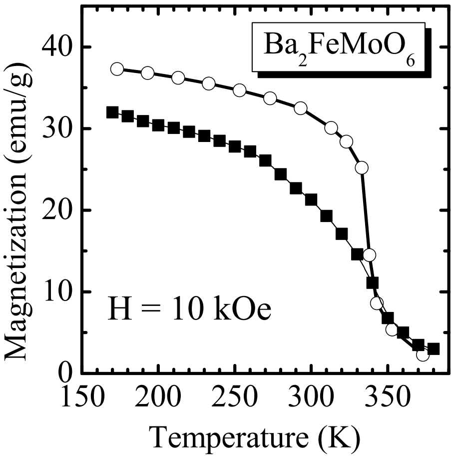

Fig. 4. Temperature dependence of magnetization (warming curves) for zero-field cooled (ZFC) Ba_2FeMoO_6. Hollow circles: sample prepared by wet chemistry; solid squares: sample prepared by solid-state reaction.

between M_0 and x, respectively, as

$$M_0(\mu_B/\text{f.u.}) = x/25 \tag{2}$$

and

$$M_0(\mu_B/\text{f.u.}) = x/20 - 1. \tag{3}$$

The nature and origin of this decrease of the magnetisation in the presence of disorder is still a matter of debate in the literature. There are two distinct ways that the net magnetisation may be reduced in the presence of antisite defects [14]. One possibility is that the disorder destroys the specific spin arrangement of Fe and Mo sublattices without any significant effect on the individual magnetic moments at these sites. This can be achieved by transforming the ferromagnetic coupling between some of the Fe sites to an antiferromagnetic coupling. Alternately, the magnetic moments at each individual site may decrease due to the different chemical environments induced by the disorder, without affecting the nature of the spin order within the Fe and Mo sublattices. The real situation may even be a combination of both these effects, with a simultaneous reduction in the magnetic moments at different sites as well as a change in the nature of the magnetic coupling between different sites.

Based on the thermodynamic theory, the entropy change, which results from the spin ordering (i.e., ferromagnetic ordering) and is induced by the variation of the applied magnetic field from 0 to H_{max}, is given by [22,23]

$$|\Delta S_M| = \int_0^{H_{\max}} \left(\frac{\partial M}{\partial T}\right) dH. \tag{4}$$

According to equation (4), the magnetic entropy change ($|\Delta S_M|$) depends on the temperature gradient of the magnetization and attains a maximum value around the Curie temperature, at which the magnetization decays most rapidly. The big advantage of the magnetization measurements is the fact that they can be carried out rather quickly, and thus they can be used to evaluate the magnetocaloric properties of potential magnetic refrigerant materials. Isothermal magnetization curves of Ba_2FeMoO_6 have been measured at various temperatures with a vibrating sample magnetometer (VSM). Figure 5 shows a part of the isothermal magnetization curves for the Ba_2FeMoO_6 prepared by wet chemistry. In our experiments, the rate of changing the magnetic field (20 Oe/s) is slow enough to get an isothermal $M \sim T$ curve. In Figure 6, we show the temperature dependence of magnetic entropy change ($|\Delta S_M|$) under an applied field of 10 kOe for Ba_2FeMoO_6. Upon 10 kOe applied field change, the maximum $|\Delta S_M|$ of Ba_2FeMoO_6 prepared by wet chemistry and solid state reaction is 1.54 and 1.09 J/kg K, respectively. The peak of the $|\Delta S_M|$ for the sample prepared by solid state reaction becomes broader. Since the molecular weight of Ba_2FeMoO_6 is very large compared with that of ABO_3-type perovskites, the magnetic entropy change per mole of atoms ($|\Delta S_M|_{mol}$) of Ba_2FeMoO_6 is rather large (0.081 and 0.057 J/mol (atoms) K). For comparison, we summarize in Table 1 the data of several typical perovskite materials that order magnetically near room temperature (>250 K).

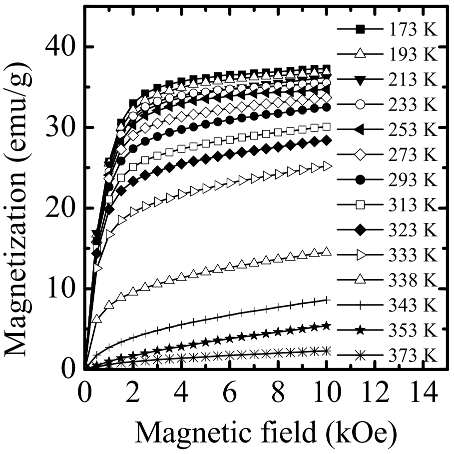

Fig. 5. Magnetization as a function of applied field measured at different temperatures for the Ba_2FeMoO_6 prepared by wet chemistry. Only a part of isothermal magnetization cures are presented.

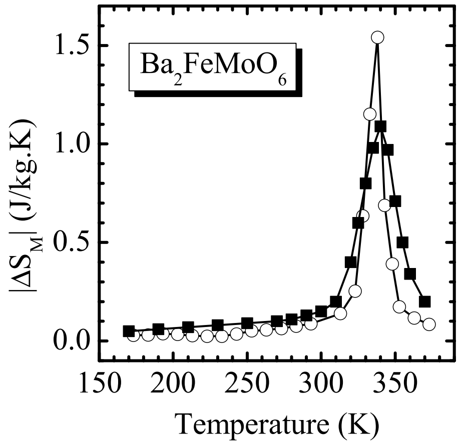

Fig. 6. Temperature dependence of magnetic entropy change in an applied field $H_{max} = 10$ kOe for Ba_2FeMoO_6. Hollow circles: sample prepared by wet chemistry; solid squares: sample prepared by solid-state reaction.

According to relation (4), a large magnetocaloric effect can be expected for materials that exhibit a sharp magnetic transition. Herein, we prepared the Ba_2FeMoO_6 using wet chemistry and synthesized at thermodynamic conditions assuring nearly ideal stoichiometry of the material with a high order parameter of the Fe and Mo arrangement. However, sample synthesized by solid state reaction showed inhomogeneous aggregates of granules with a high AS defect concentration, which negatively affects the sharpness of the magnetic transition and gives rise to a low $|\Delta S_M|$.

4 Conclusions

The structure, morphology and magnetic properties (including magnetocaloric effect) of double perovskite Ba_2FeMoO_6 prepared by wet chemistry have been compared with those of sample synthesized by solid state

Table 1. Room-temperature magnetic entropy change ($|\Delta S_M|$ and $|\Delta S_M|_{mol}$) of perovskite-type materials at their Curie temperature (>250 K) in low magnetic fields.

Sample	T_C (K)	ΔH (×10 kOe)	$\lvert\Delta S_M\rvert$ (J/kg K)	$^a\lvert\Delta S_M\rvert_{mol}$ (J/mol (atoms) K)	Source of Data
Ba_2FeMoO_6 [b]	340	1.0	1.54	0.081	Present work
Ba_2FeMoO_6 [c]	340	1.0	1.09	0.057	Present work
$La_{2.061}K_{0.935}Mn_{1.997}O_7$	254	1.0	1.1	0.050	[24]
$La_{2/3}Ba_{1/3}MnO_{3.00}$	337	1.0	2.77	0.134	[25]
$La_{0.834}Na_{0.163}Mn_{1.000}O_3$	343	1.0	2.11	0.094	[26]
$La_{0.796}K_{0.196}Mn_{0.993}O_3$	344	1.0	1.55	0.068	[26]
$La_{0.75}Sr_{0.15}Ca_{0.10}MnO_3$	327	1.5	2.8	0.126	[27]
$La_{0.75}Sr_{0.125}Ca_{0.125}MnO_3$	283	1.5	1.5	0.068	[27]
$La_{0.65}Ca_{0.35}MnO_3$	~255	1.0	~2.7	0.112	[28]
$La_{0.67}Ca_{0.33}MnO_\delta$	260	1.0	1.1	0.046	[29]

[a] molar magnetic entropy change calculated from $|\Delta S_M|$;
[b] prepared by wet chemistry;
[c] prepared by solid state reaction.

reaction. The use of wet chemistry method enables the formation of double perovskite Ba_2FeMoO_6 containing high aspect ratio crystallites with a high order parameter of the Fe and Mo arrangement. The sample prepared by wet chemistry exhibits a large magnetization, a sharp magnetic transition and a large magnetic entropy change under a low magnetic field above room temperature. Although the properties of our materials are far from optimal, further exploration of this double perovskite may prove fruitful.

This work is supported by the National Natural Science Foundation of China under Grant No.50072007, and the National Key Project for Basic Research (No. G1999064508), People's Republic of China.

References

1. K.I. Kobayashi, T. Kimura, H. Sawada, K. Terakura, Y. Tokura, Nature **395**, 677 (1998)
2. LI. Balcells, J. Navarro, M. Bibes, A. Roig, B. Martínez, J. Fontcuberta, Appl. Phys. Lett. **78**, 781 (2001)
3. M. Itoh, I. Ohta, Y. Inaguma, Mater. Sci. Eng. B **41**, 55 (1996)
4. A.S. Ogale, S.B. Ogale, R. Ramesh, T. Venkatesan, Appl. Phys. Lett. **75**, 537 (1999)
5. J. Navarro, J. Nogue's, J.S. Muñoz, J. Fontcuberta, Phys. Rev. B **67**, 174416 (2003)
6. Y. Moritomo, S. Xu, A. Machida, T. Akimoto, E. Nishibori, M. Takata, M. Sakata, Phys. Rev. B **61**, R7827 (2000)
7. J. Navarro, C. Frontera, L.I. Balcells, B. Martínez, J. Fontcuberta, Phys. Rev. B **64**, 092411 (2001)
8. J. Navarro, LI. Balcells, F. Sandiumenge, M. Bibes, A. Roig, B. Martínez, J. Fontcuberta, J. Phys.: Condens. Mater **13**, 8481 (2001)
9. S.B. Kim, B.W. Lee, S.R. Yoon, C.S. Kim, J. Magn. Magn. Mater. **254–255**, 580 (2003)
10. D. Niebieskikwiat, A. Caneiro, R.D. Sanchez, J. Fontcuberta, Phys. Rev. B **64**, 180406 (2001)
11. B.G. Kim, Y.S. Hor, S.W. Cheong, Appl. Phys. Lett. **79**, 388 (2001)
12. D.D. Sarma, P. Mahadevan, T. Saha-Dasgupta, S. Ray, A. Kumar, Phys. Rev. Lett. **85**, 2549 (2000)
13. J. Linden, T. Yamamoto, M. Karppinen, H. Yamauchi, T. Pietari, Appl. Phys. Lett. **76**, 2925 (2000)
14. D.D. Sarma, Current Opinion in Solid State and Mater. Sci. **5**, 261 (2001)
15. H.Yanagihara, W. Cheong, M.B. Salamon, S. Xu, Y. Moritomo, Phys. Rev. B **65**, 092411 (2002)
16. G. Popov, M. Greenblatt, M. Croft, Phys. Rev. B **67**, 024406 (2003)
17. C.L. Yuan, Y. Zhu, P.P. Ong, Appl. Phys. Lett. **82**, 934 (2003)
18. K. Phillips, A. Chattopadhyay, A.J. Millis, Phys. Rev. B **67**, 125119 (2003)
19. R.P. Borges, R.M. Thomas, C. Cullinan, J.M.D. Coey, R. Suryanarayanan, L. Ben-Dort, L. Pinsard-Gaudart, A. Revcolevschi, J. Phys.: Condens. Mater **11**, L445 (1999)
20. Y. Tomioka, T. Okuda, Y. Okimoto, R. Kumai, K.I. Kobayashi, Y. Tokura, Phys. Rev. B **61**, 422 (2000)
21. H. Sakuma, T. taniyama, Y. Kitamoto, Y. Yamazaki, J. Appl. Phys. **93**, 2816 (2003)
22. V.K. Pecharsky, K.A. Gschneidner Jr, J. Magn. Magn. Mater. **200**, 44 (1999)
23. V.K. Pecharsky, K.A. Gschneidner Jr, J. Appl. Phys. **90**, 4614 (2001)
24. W. Zhong, W. Chen, H.Y. Jiang, X.S. Liu, C.T. Au, Y.W. Du, Eur. Phys. J. B **30**, 331 (2002)
25. W. Zhong, W. Chen, C.T. Au, Y.W. Du, J. Magn. Magn. Mater. **261**, 238 (2003)
26. W. Zhong, W. Chen, W.P. Ding, N. Zhang, A. Hu, Y.W. Du, Q.J. Yan, Eur. Phys. J. B **3**, 169 (1998)
27. Z.B. Guo, Y.W. Du, J.S. Zhu, H. Huang, W.P. Ding, D. Feng, Phys. Rev. Lett. **78**, 1142 (1997)
28. X. Bohigas, E. del Barco, M. Sales, J. Tejada, J. Magn. Magn. Mater. **196**, 455 (1999)
29. X.X. Zhang, J. Tejada, Y. Xin, G.F. Sun, K.W. Wong, X. Bohigas, Appl. Phys. Lett. **69**, 3596 (1996)